A029

Horizontal Simulation Grids as Alternative to Structure-based Grids for Thin Oil-zone Problems

O. Pettersen* (University of Bergen)

SUMMARY

As a general rule, the layering in reservoir simulation grids is based on the geology, e.g. structure tops. In this paper we investigate the alternative of using horizontal layers, where the link to the geology model is by the representation of the petrophysics alone. The obvious drawback is the failure to honor the structure in the grid geometry. On the other hand a horizontal grid will honor the initial fluid contacts perfectly, and horizontal wells can also be accurately represented. Both these issues are vital in thin oil-zone problems, where horizontal grids may hence be a viable alternative.

To investigate this question, a number of equivalent simulation models were built for a segment of the Troll Field, both geology-based and horizontal, and various combinations of these. In the paper it is demonstrated that the horizontal grid is able to capture the essentials of fluid flow with the same degree of accuracy as the geology-based grid, and near-well flow is considerably more accurate. For grids of comparable resolution, more reliable results were obtained by a horizontal grid than a geo-grid. A geo-grid with local grid refinement and a horizontal grid produced almost identical results, but the ratio of computing times was more than 20 in favor of the horizontal grid. In the one-phase regions of the reservoir, relatively coarse cells can be used without significant loss of accuracy.

Introduction

The Troll Field is situated about 60 km west of the Norwegian West coast, at approx. 300 m water depth, and is operated by Statoil. It is primarily a gas field, but also contains a thin oil zone with thickness varying from zero to 26 m. The use of horizontal wells has resulted in a successful recovery of this oil zone, which initially was regarded as challenging to produce due to coning and cusping of both water and gas – typical for thin oil zone production (Fantoft, Krogh, Pollen, 1988; Lien, Seines, Havig, and Kydland, 1991; Seines, Lien, and Haug, 1994; Thakur, Bally, Therry, and Simon, 1996; Kabir, Agamini, and Holguin, 2004).

Simulation of the Troll oil zone also represents a challenge, due to the combination thin oil zone and huge areal extent. A high-resolution grid is needed to capture fluid movement in the vicinity of the producing wells, while the size of the field prohibits such a grid field-wise. One successful compromise was presented by Henriquez, Apeland, Lie, and Cheshire (1992), where they used local grid refinement (LGR) surrounding the wells and vertical equilibrium (VE) outside the LGR areas. Although good results were achieved there was (and still is) some uncertainty tied to the accuracy of the VE-to-LGR flow. In addition, the simulations were time-demanding, and were implemented on a parallel architecture (Bowen and Leiknes, 1995).

An alternative approach is the use of horizontal grids (*hor-grids*), which is the topic of this paper. The majority of simulation grids used in the oil industry honors the geological structural model and petrophysics by ensuring that the simulation grid layers coincide with the structure tops or sequence stratigraphic tops. Such grids will be called *geo-grids* in this paper. A horizontal grid on the other hand is comprised of horizontal layers, which obviously bear no relation to the geology. The main argument for proposing this type of grid is that while the geo-grid is able to capture geological and petrophysical variation relatively accurately, the fluid contacts in general are horizontal, and hence contact movement may be better resolved on a horizontal grid. In a thin oil zone setting the high-resolution part of the grid can be confined to the dynamic three-phase domain, roughly from somewhat above the initial gas-oil contact (GOC) to somewhat below the initial oil-water contact (OWC), which is a relatively small volume compared to the entire reservoir. In the gas and water zones, away from the contacts, the flow is essentially one-phase and can probably be adequately described with lower resolution. In contrast, the oil zone can pass through most or all formations in a dipping reservoir, such that it is not possible to limit the high resolution part of the grid in the same fashion. A priori the intuitive benefits and drawbacks of the two alternative grids can be summarized in **Table 1**.

TABLE 1—BENEFITS AND DRAWBACKS OF GEO-GRID VS: HOR-GRID: A PRIORI INTUITIVE FEELING

	Geo-grid	**Hor-grid**
Geological layering	Accurate	Only implicit
Petrophysics	Honors data	Approx. honors data
Fluid contacts	Approximate	Accurate
Contact movement	Approximate	Expected better
Well completions	Approximate	Can be accurate
General fluid flow	Simulator quality	Open question, topic of this paper

The main disadvantage of a horizontal grid is the lack of alignment to the structural model, which historically has been seen as highly desired. (Whether this is a real or conceived drawback is attempted resolved in this paper.)

Provided the quality of the simulated fluid flow is acceptable on a horizontal grid, this kind of grid also has some computational advantages;

- The oil zone can be modeled with sufficiently thin layers, which can be confined to the oil zone alone, and hence does not increase the total number of cells significantly (high resolution only where needed).
- As all cell top / bottoms are horizontal, cell shapes will be regular, hence better suited for numerical computations.

- All cell-to-cell connections are regular, even across faults. (No non-neighbor connections (NNCs) in corner-point grid terminology).

Horizontal grids were used to model near-well flow on Troll already in the beginning of the 1990's. During the last few decades such grids have been used in different contexts and with apparent success, e.g. Hsu (1998); Kabir, Agamini, and Holguin (2008). However, such models were used as *ad hoc* tools, and no attempts were made to assess the quality of the horizontal grid models versus traditional geo-grids.

When Norsk Hydro AS (later Statoil) decided to build a new generation of Troll oil zone simulation models, it was determined to test and compare the performance of different kinds of gridding approaches on a representative segment of the field. The goal was to identify the strategy that would provide the best combination of reliable results and affordable computing time.

The Troll sands include an alternating pattern of dipping clean, high-permeability sands (C-sands) interbedded with micaceous and silty to fine-grained sands of significantly lower permeability (M-sands). Calcite cementation occurs in all lithologies over the entire field. The production scenario is to a large extent based on the principle of placing the horizontal wells in C-sands, slightly above the OWC, such that the M-sands may act as partial barriers to gas inflow from above. An important aspect of the horizontal grid is therefore the ability to reproduce the interbedding of C- and M-sands, and capture the gas flow pattern from the gas zone to the well perforations, as well as the fluid contacts movement through time.

Geo-grids and Horizontal Grids

The horizontal grids in this paper were constructed by purpose-developed software, by direct sampling and rescaling of an existing geo-grid. I.e., the areal definition of the grid is left unchanged by the conversion, as well as the vertical alignment of cell corners. (In corner point terminology, the coordinate lines from the geo-grid are used unaltered in the hor-grid.) For best results, the geo-grid should have as high vertical resolution as possible, optimally in one-to-one correspondence with the geological model.

The hor-grid can be either a pure horizontal grid, or a hybrid grid (combination of geo-based and horizontal layers. A general description of the target grid is,

1. Top and bottom cut-off depths
2. n_T geo-based layers in the upper geo-grid zone.
3. n_H horizontal layers in the hor-layers zone.
4. n_B geo-based layers in the lower geo-grid zone.

The cut-off depths are usually set to the shallowest and deepest point in the reservoir, such that the entire reservoir is included in the grid. A true horizontal grid is obtained when $n_T = n_B = 0$, else a hybrid grid results.

Figs. 1–5 show examples of the different kinds of grid, including the permeability in the *x*-direction.

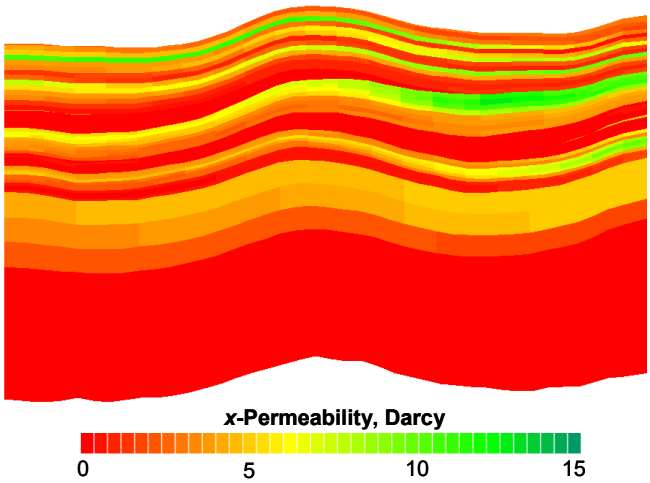

Fig. 1. Vertical cross-section of original geo-grid

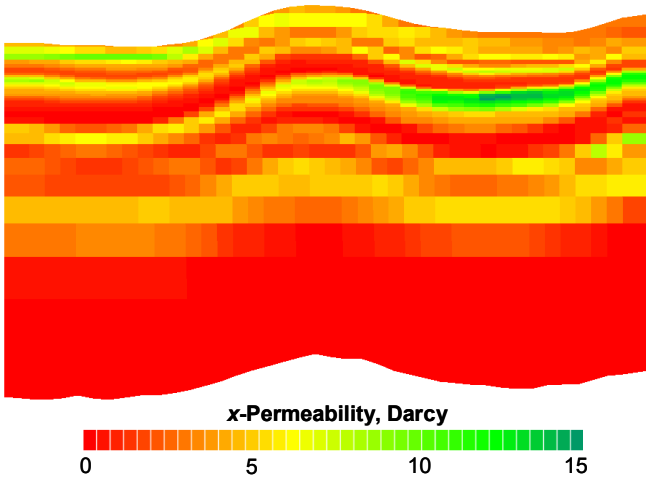

Fig. 2. Cross-section as in Fig. 1, true horizontal grid

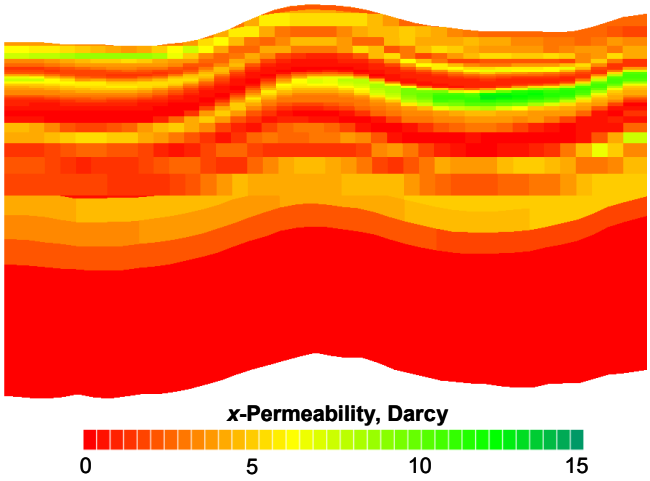

Fig. 3. Cross-section as in Fig. 1, hybrid grid

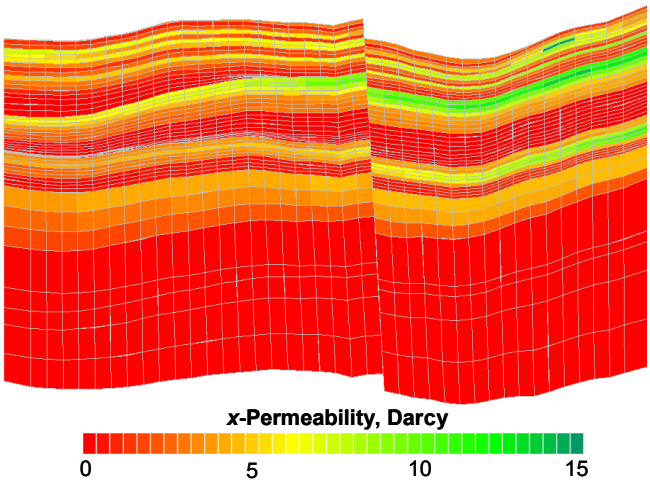

Fig. 4. Vertical cross-section including a fault, geo-grid

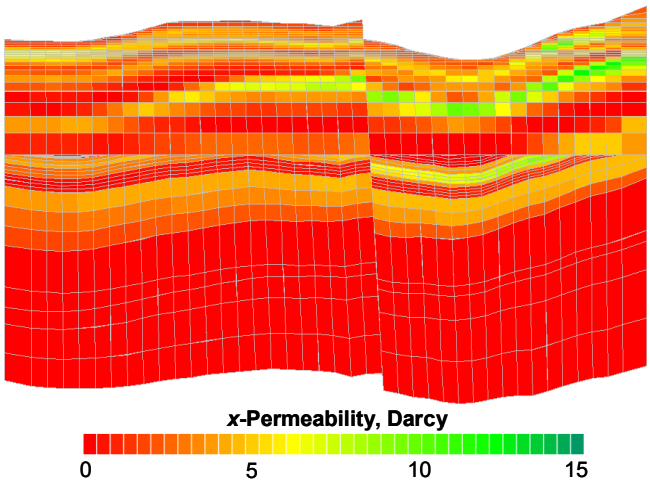

Fig. 5. Cross-section as in Fig. 4, hybrid grid

Note the handling of the fault in Figs. 4–5. In the geo-grid, faults are geometrical discontinuities, which result in non-neighbor connections in a corner-point grid. In the horizontal grid, the fault is represented as a discontinuity in the petrophysics only – all connections between grid cells across the fault are regular.

Note also the representation of the high, respective low permeability zones. It is imperative that sand continuity is conserved in the horizontal grid for such zones.

Rescaling Geo-grid → Hor-grid

As the grid cell sizes in the geo-grid and the horizontal grid normally are of the same order of magnitude, mapping of parameters from the geo-grid to the horizontal grid is relatively straightforward, with a possible exception for the permeabilities. For completeness we describe the rescaling procedure.

In any cell, its areal indices (i and j) will be the same on the geo-grid and the hor-grid. For the vertical index we use K for the geo-grid layer, and k for the hor-grid layer.

Looking at cell (i, j, k) in the horizontal grid, in the general case N geo-grid layers ($K = K_1, K_2, \ldots K_N$) will pass through the cell, as in **Fig. 6**.

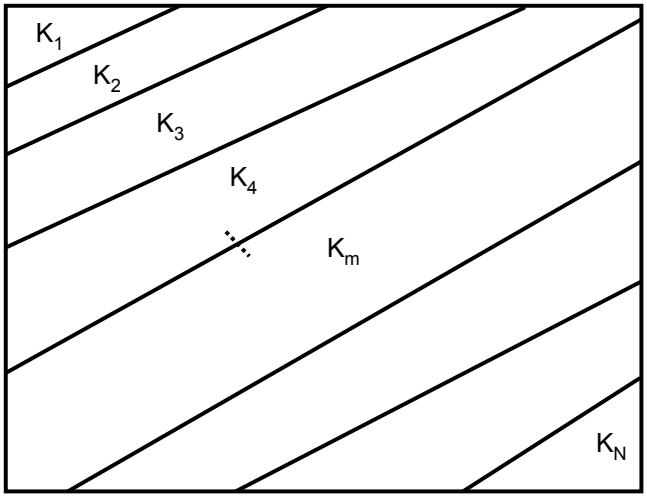

Fig. 6. Example of a horizontal grid cell, with *N* geo-grid layers passing through the cell

First the volumes of the part of the geo-layers that belong to the horizontal cell are evaluated, $V_1, V_2, \ldots V_N$. Integer variables (typically fluid-in-place regions and other defined regions) are taken as the

value belonging to the maximum of the V_m, $m=1,...,N$. Properties requiring arithmetic average (porosity, net-to-gross) are computed as standard volume-weighted averages.

Rescaling of permeability

Horizontal permeability K_h is generally understood as the permeability in the direction along the layer, as the vector KX^{Geo} in **Fig. 7**. This is also in agreement with the computational scheme, as e.g. flow between cells (i, j, K) and $(i+1, j, K)$ is based on the transmissibility between the cells, which is along the layering. On a horizontal grid, the corresponding cells are true horizontal neighbors, such that the transmissibility in question is based on true horizontal permeabilities, independent of the dip angle of the geological layering. The rescaling of permeabilities must account for this. We explain the calculation of x-permeability KX in one horizontal cell. The first stage is to compute the horizontal projections of KX^{Geo}, KY^{Geo}, and KZ^{Geo}, for all layers $K_1, K_2, \ldots K_N$ (Fig. 6). Then the horizontal x-permeability in one of the geo-layers (KX^{Hor}) (Fig. 7) is the sum of the projections of KX^{Geo}, KY^{Geo}, and KZ^{Geo} along the x-axis.

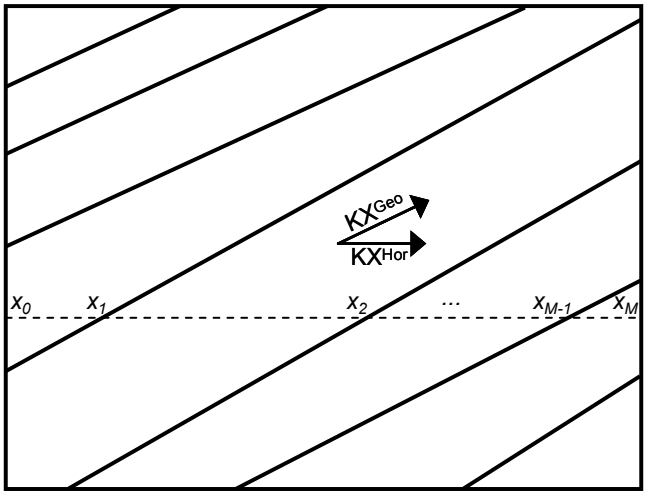

Fig. 7. Computing of true horizontal permeability. Notation

It is well known that the appropriate permeability average for flow transverse to a permeability variation is the harmonic average, while the arithmetic average is appropriate for flow parallel to the variation. Hence, we first compute the inline horizontal permeability as the harmonic average across the geo-layers, along the dashed line in Fig. 7, where the x_i are the geo-layer boundaries;

$$\frac{x_M - x_0}{KX^{Hor}_{inline}} = \int_{x_0}^{x_M} \frac{dx}{KX^{Hor}(x)} = \sum_{m=1}^{M} \frac{x_m - x_{m-1}}{KX^{Hor}_m}$$

Then the final horizontal cell x-permeability is computed as the arithmetic average of the inline KX^{Hor} (volume-weighted sum over all present geo-layers). This scheme has intuitive appeal: As vertical permeability in general is smaller than horizontal the flow in Fig. 6 will be mainly along the geo-layering (in the KX^{Geo}-direction). For horizontal cells this preferred flow direction is lost by the re-gridding if permeabilities are naïvely copied from the geo-grid. The permeability calculations presented above will typically reduce the x-permeability and increase the z-permeability when mapped from geo-grid to hor-grid. This alters the flow-direction preference done by the numerical scheme from horizontal to more diagonal, in agreement with the original layering.

Inter-layer transmissibility multipliers

Thin, low permeability barriers (e.g. shale) are often represented by vertical transmissibility multipliers in grids. ("MULTZ" in ECLIPSE terminology (Schlumberger, 2009)) During the conversion to horizontal layers each (geo-)MULTZ is transformed to a set of MULTX, MULTY, and MULTZ parameters that cover the corresponding area in the horizontal grid, assuring that continuity is not lost.

Fault transmissibility multipliers
As mentioned earlier, faults in the geo-grid are geometry discontinuities, most often accompanied with fault transmissibility multipliers to honor the fault volume permeability. The defined multipliers are mapped directly to the associated cells in the horizontal grid. Hence, a fault in the horizontal grid will be geometry continuous (as the grid is completely regular), but the flow restrictions will be taken care of by parameter discontinuities and transmissibility multipliers (Fig. 5).

Base Model 1: BASEGEO

To get as reliable results as possible from the base models, relatively fine meshes were used, with horizontal cell diameters *(Δx, Δy)* of 40–50 m. In the basic geo-grid, denoted **BASEGEO**, the layering was taken directly from the structural geo-model for the segment, with 56 layers. The grid comprises 40 x 40 x 56 cells (89600 total), of which 81403 are active. 2270 non-neighbour connections (NNCs) are present (see Figs. 1 and 4 for examples of cross-sections).
Total model thickness is about 200 m, whereof the gas cap is about 40 m thick, the oil zone is 13 m, and the remaining ~160 m is water. Cells which are less than 0.1 m thick have been set inactive.

For petrophysics and fluid data representative Troll data have been used.

Wells
The key question in this study is how fluid front movement is tracked by the two different approaches, geo-grid and hor-grid. The wells have been selected with this question in mind.
Four vertical water-injectors were placed in the corners of the grid, injecting into the lower parts of the reservoir. A horizontal gas injector was placed parallel to the SW edge near the top (layer 2). The horizontal oil producers were defined as true horizontal, 0.5 m above the OWC. All were placed such that they spanned an interval of high-permeable sand. The main reason for this was that we would then have an a priori physical intuition of the qualitative shape of the gas production development (ref. "Run Series 1" section below). The well positions are shown in **Fig. 8**, which is a slice through the grid at producer-depth (the gas injector and water injectors are at different depths from this slice). Also shown is the permeability distribution at producer depth. The perforations were defined in the cells with cell centre closest to true target depth.

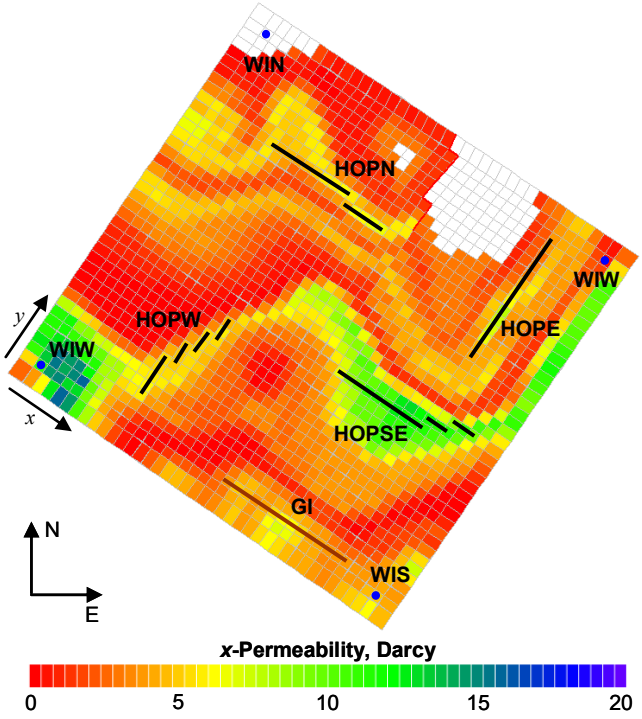

Fig. 8. Grid slice at producer depth, showing all wells

The producing and injecting target rates were attempted set such that actual pressure depletion rate of the field would be (coarsely) reproduced. Once appropriate target rates had been determined, the schedule was kept unchanged in all runs.

Base Model 2: BASEHOR

The basic horizontal grid, **BASEHOR**, uses the same set of coordinate lines as BASEGEO, hence the area cell resolution is unchanged.

In many of the horizontal grids that were constructed in this study the layer thicknesses ΔZ were defined by a geometric increase factor m. Typically ΔZ will increase from the GOC upwards and from the OWC downwards, such that if a layer has thickness ΔZ, the layer above (gas) or below (water) will have thickness $m \cdot \Delta Z$.

The horizontal grid definition is,

- The oil zone: 13 layers, each 1 m thick
- From GOC upwards 8 horizontal layers were defined, with geometric increase factor m = 1.25. The total thickness of the horizontal layers in the gas cap is 24.5 m.
- From OWC downwards 10 horizontal layers were defined, with m = 1.25. Total thickness of the water zone horizontal grid is 41.5 m.
- Above and below the horizontal grid interval, the geo-layers from the BASEGEO model have been kept, with a total of 10 geo-layers in the top of the reservoir, and 35 geo-layers at the base.

Summing up grid definition top-down:

- Top 18 m: 10 geo-layers
- Next 79 m: 31 horizontal layers
- Bottom 124 m: 35 geo-layers
- 76 layers in total
- Number of cells: 121600
- Number of active cells: 63774
- Number of NNCs: 865

Ref Figs. 3, 5, and 8.

Petrophysics, regions and fault multipliers were resampled to the horizontal grid as described in the “Rescaling” section above.

The water and gas injectors were defined to match the perforation positions from the BASEGEO model as closely as possible, while all the horizontal producers were defined at their true depth. (The horizontal grid definition ideally should be such that the relevant cell centre depths match the perforation depths exactly. Hence, for a horizontal well with an undulating well path, the grid should be adjusted such that all perforations are at cell centers.)

Base Model 3: GEOLGR

Intuitively, and by experience from previous Troll simulation models, near-well simulated flow and production can be improved by using local grid refinement in the vicinity of the horizontal producers. For comparison, the case **GEOLGR** was built as a local grid refinement extension to the BASEGEO case. In the GEOLGR grid, a volume surrounding each well path has been defined with local refined cells (each coarse cell comprises 3 x 3 x 3 LGR cells),

- Areally, the LGR was defined on a box which included the well path and one extra row of coarse cells on each side of the (coarse) well cells.
- Vertically, the layers to refine were chosen by a similar criterion, the LGR should cover all layers which contained perforations, and an extra (coarse) layer above and below.
- Total number of active global cells: 81344
- Total number of active local cells: 129336
- Total number of active cells: 210680
- Number of NNCs: 2270

Run Series 1: Horizontal vs. Geo-grid

The purpose of the first series of runs was to compare the results from the different gridding scenarios (BASEGEO, BASEHOR, and GEOLGR). Naturally, we don't have available "correct" results with which to compare, so we need to use other criteria to assess the quality.

Firstly, the way the wells have been defined, all producers are parallel to the GOC. Moreover, all producers were placed in a high-permeable sand, such that this sand layer extends all the way to the GOC as a clean, homogeneous high-conductive sand. I.e. for a given well, the distance up to the GOC, measured along the high-permeable sand is identical for all perforations. Hence we should expect simultaneous gas breakthrough in all perforations, and after breakthrough the gas-oil-ratio (GOR) should rise quickly to its maximum value. Note however that wells HOPN and HOPE has no or only a small gas cap above, so gas production from these wells should be expected to be less predictable, since it will be caused by a more complex gas flow pattern.

Secondly, we will use a standard iterative approach; when we change the data deck only incrementally in a manner that is obviously an improvement, we expect an incremental improvement in the solution. This argument has however some limitations, as e.g. when we reduce grid cell sizes, an improved solution is intuitively expected. On the other hand this can lead to reduced numerical accuracy, so the net gain / loss can be difficult to identify.

A number of initial runs were performed to test various scenarios, for sensitivity studies, and to gain knowledge of the general behavior. Following this trial stage an extensive test scheme was set up. From this scheme, only a few figures documenting key results will be reported. Note that the conclusions which are stated in the text are typically based on observed behavior from a large number of runs, although only an excerpt of these runs are described by text or figures in the paper.

Field (total) production results.

Simulated oil production was as good as equal in the three base cases (within expected uncertainty). Water rates differed in that the BASEGEO case predicted a little earlier water breakthrough than the other two cases, but the total (cumulative) produced water was for practical purposes equal. The largest differences were seen in the gas production, **Figs. 9–10**. The BASEGEO case is here significantly different from the other two cases. Also note the rate oscillations for the GEOLGR case, which is an (unfortunate) feature of large LGR models. (The GEOLGR case was terminated prematurely due to max permitted CPU time (100000 seconds). Although the case could have been rerun, this was not done as the run contained sufficient information to be of value as a comparison.)

Reservoir pressure is very sensitive to the gas production, but the depletion rate was attempted preserved as good as possible between runs. The pressure trend differs somewhat between the cases after gas breakthrough, with BASEGEO following a different trend than GEOLGR and BASEHOR, which were relatively equal.

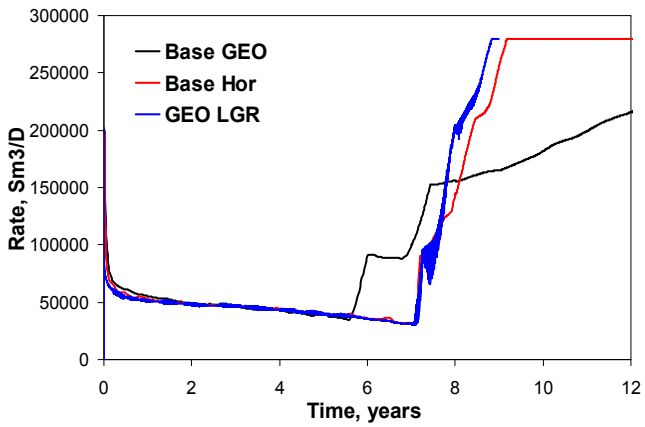

Fig. 9. Field (total) gas production rate from the three base cases

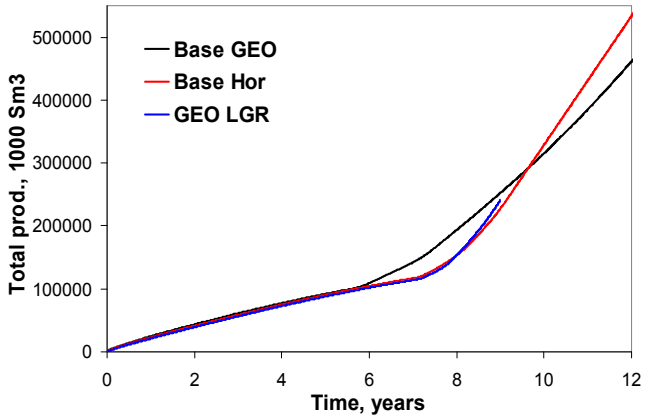

Fig. 10. Field cumulative gas production from the three base cases

Well production results

Oil rates, and especially cumulative production were comparable in the three cases. In general, where (slight) differences were present, the BASEGEO case was the deviating case, while BASEHOR and GEOLGR were relatively equal. The same observation applies also to water rates and water production, with BASEGEO differing more significantly from the other two cases.

As a priori expected, the well gas rates are where the largest differences between the three cases are seen. The behavior seen in **Fig. 11** (gas rate from well HOPW) is representative for all the wells. As mentioned earlier, by the model set-up the gas rate should have an abrupt and considerable rise after gas break-through. This has been captured by the BASEHOR and GEOLGR cases, but not by the BASEGEO. Generally, in all results concerning gas production from wells the BASEHOR and GEOLGR cases were similar or equal, while the BASEGEO case deviated significantly – also from expectations by physical intuition.

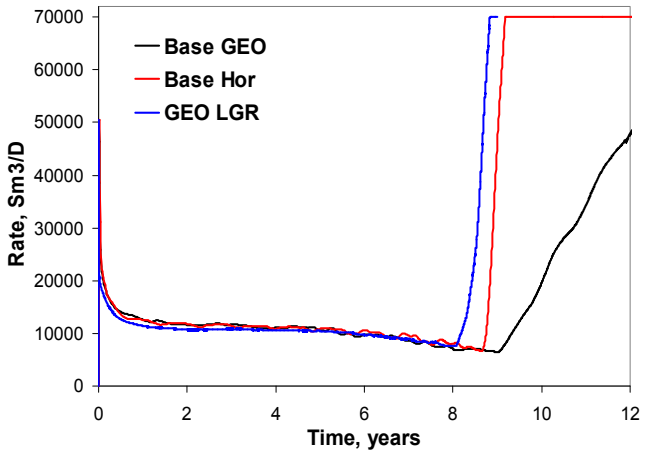

Fig. 11. Gas rate from well HOPW from the three base cases

Fluid contact movement

By comparing the fluid front movement near the contacts (especially the GOC) it was found that apart from the difference in resolution, the three cases in question had relatively equal behaviour (subjective conclusion by comparing saturation states in a 3-D graphics program). To test this further, some LGR-cases were constructed from the BASEGEO model with local grid refinement near the initial fluid contacts, in the upper parts of the oil zone, or covering most of the oil zone and gas cap. (It was essential not to use LGR in the horizontal well vicinity in this part-study.) The results from these runs were qualitatively equal to the BASEGEO-results, and differed noticeably from BASEHOR and GEOLGR. Hence, different resolution in the contact movement zone cannot explain the differences between BASEGEO and BASEHOR / GEOLGR.

Summary Series 1
BASEGEO is unable to capture expected gas production (from physical intuition), while BASEHOR and GEOLGR both appear to succeed in this respect, and as the two runs also generally are in agreement, it is tempting to conclude that they are closer to reality than BASEGEO. The differences are not tied to fluid contact movement, but rather the well modeling. It is therefore of interest to address this topic closer.

Run Series 2: Completion modeling

In a simulation grid well perforations cannot be defined at their exact position, but are represented at the cell centre of the grid cell which contains them. In this context it is apparent that due to the short distance from the fluid contacts to the perforations, a small error in perforation depth may have large consequences. As the differences in e.g. gas rates as seen in Fig. 11 could not be explained by inaccuracies in the simulated fluid contact movement it is natural to investigate the significance of the perforation modeling.

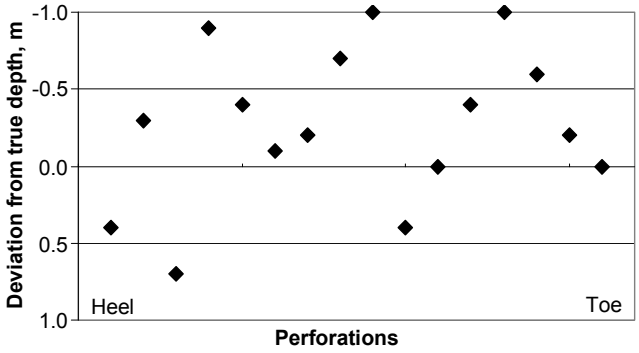

Fig. 12. Difference between modeled and true perforation depths, case BASEGEO, well HOPSE

Fig. 12 is a schematic of how the perforation depths in well HOPSE were represented on the grid. Note that the deviations are not large; on this grid with cell diameters 40–50 m the error is in the range ±1 m. To test if such small deviations has noticeable influence three sensitivity cases of BASEGEO were run:

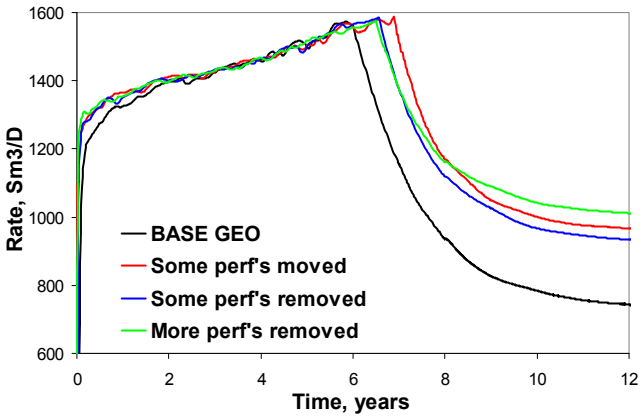

Fig. 13. Water prod. rate well HOPSE, BASEGEO with sensitivities on perforation positions

1. All perforations which were above true perforation depth in BASEGEO were moved to the cell directly below
2. All perforations which were more than 0.7 m above true perforation depth in BASEGEO were removed

3. As (2), but the cutoff distance was 0.25 m

Some results from this series can be seen in **Figs. 13–14**.

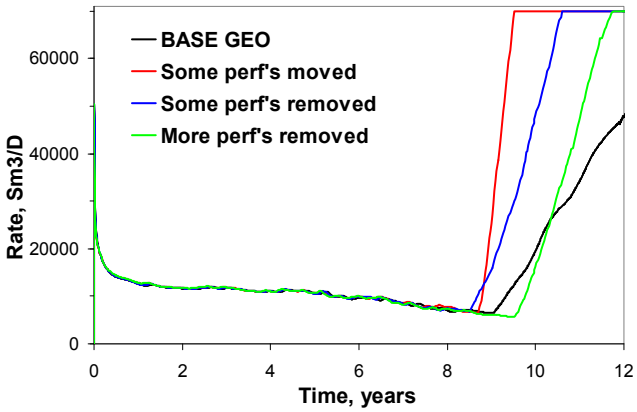

Fig. 14. Gas prod. rate well HOPW, BASEGEO with sensitivities on perforation positions

Clearly, these runs confirm that even a small change in modeled perforation depth has strong influence on the results. Hence it can be concluded from these sensitivities that correct perforation depths is a critical factor in thin oil-zone simulations. In Fig. 14 the simulated gas break-through differs by almost two years due to less than one meter inaccuracy in modeled perforation depths. Note also that the BASEGEO model has smaller cell sizes than would be possible in a full field model, such that the perforation depth errors on a geo-grid typically will be considerably larger. (On the GEOLGR model the perforation error was within ±0.5 m. However, in a realistic-size model the LGR cells would probably be at least as large as the cells in the BASEGEO model.)

Summary of Series 1 and 2 runs

- Fluid frontal movement is adequately described in all three base models (BASEGEO, BASEHOR, GEOLGR)
- The BASEGEO model fails to capture essentials of gas flow near the producing wells. To a lesser degree the same applies to water flow
- The GEOLGR and BASEHOR models were able to capture much of the same features with comparable results. Simulated results were more in accordance with physical intuition than BASEGEO
- One benefit of the BASEHOR model compared to the other two is that the high resolution cells can be concentrated to the domains where they are most needed
- The GEOLGR model suffers from partly severe rate oscillations

Hence the horizontal grid model appears to be able to deliver results at least as good as local grid refinement, and considerably better than the traditional geo-grid model.

When comparing computing times, the advantage of the horizontal grid model becomes even clearer.

Computing times (CPU) for the three base cases:

BASEGEO 183 min
BASEHOR 133 min
GEOLGR 2920 min (estimated)

(As mentioned above the GEOLGR case was prematurely terminated after 1667 minutes)

Run Series 3: Grid Coarsening

The cell sizes chosen in the runs described above were unrealistically small, to enable construction of a reliable reference case. For real-size or full field models cell sizes will be larger, and in this batch of runs the significance of cell size is investigated. As there is no reason to believe that a larger-cell geo-

grid will perform any better than the BASEGEO case, the test was performed with horizontal grids only.

Two new grids were constructed, with cell diameters twice and three times the GEOGRID diameters respectively. First new geo-grids with the updated cell sizes were made (keeping the original layering). Then new horizontal grids were constructed from these, using the same (horizontal) layering scheme as in the BASEHOR case.

Some results are shown in **Figs. 15–16**.

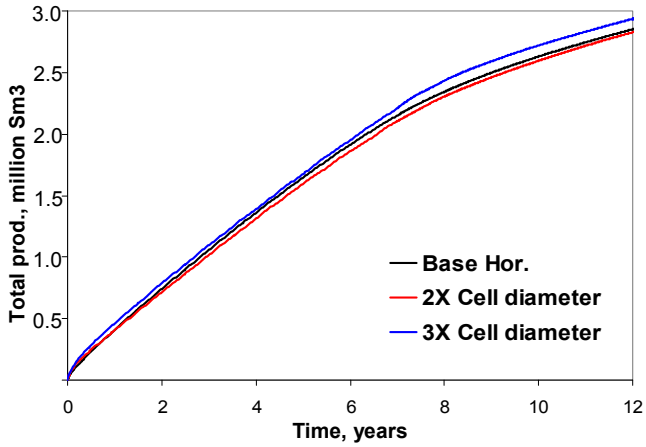

Fig. 15. Field total (cumulative) oil production, hor-grids with different cell sizes

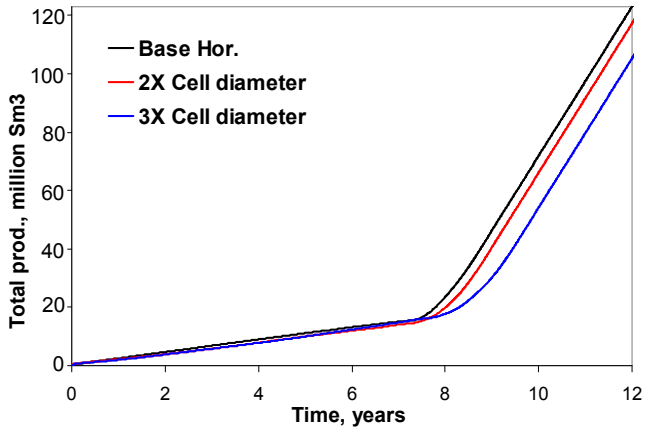

Fig. 16. Total (cumulative) gas production from well HOPE, hor-grids with different cell sizes

In general the difference between these three cases were not significantly large. Field production of all three phases and reservoir pressure are equal within expected uncertainty (Fig. 15). At well level water production is identical, while there are some small differences in gas production (Fig. 16). The 3X diameter case can in some sense be regarded as representing the point where coarsening effects start to be of significance, hence we can conclude that a cell diameter of 100–150 m is sufficiently fine to preserve accuracy in the results.

As the preceding arguments have shown that it is sufficient and necessary to use high resolution cells in the dynamic domains (especially near wells), a valid approach would be to use a relatively coarse hor-grid model with LGRs in chosen areas. Such grids are intuitively attractive (probably optimal), but have not been studied in this paper.

CPU times for the three levels of coarsening:

BASEHOR	133 min
HOR 2X Cell diameter	8 min 34 sec
HOR 3X Cell diameter	2 min 34 sec

As the results obtained from the three cases were relatively equal, there is evidently a lot to gain in efficiency by using coarser cells.

Run Series 4: Optimizing the hor-grid

Once the decision to use a horizontal grid has been taken, the next question to be addressed is how to define the horizontal layering in an optimal manner. To this extent a number of test cases were run, all using the "2X diameter" grid, and a summary of the results are presented in this section. To enable presentation of the conclusions in a concise form, a total variation variable *TV* will be used. Of the close to 100 cases that were run, one was chosen as a reference case (one resembling the BASEHOR case). The results to base the comparisons on were chosen as well rates for oil, water, and gas for all wells: the result vector *RV* is the set {oil rate, water rate, and gas rate from wells HOPN, HOPE, HOPSE, and HOPW}.

Then, using R_V to denote (normalized) results from the reference case, and r_V for corresponding results from the comparison case,

$$TV = \frac{1}{N} \sum_{V \in RV} \sum_{t=1}^{N} [r_V(t) - R_V(t)]^2 \qquad (1)$$

where *t* denotes the time variable, taken at 15-day intervals, and *N* is the number of time steps. The total variation is hence the square difference between the comparison and reference cases, summed for all report steps and all relevant result vectors.

The *TV* is "just a number", but from experience, cases with *TV* less than unity are "as good as equal", while noticeable differences begin to appear for $TV \approx 2$. An example is shown in **Fig. 17**.

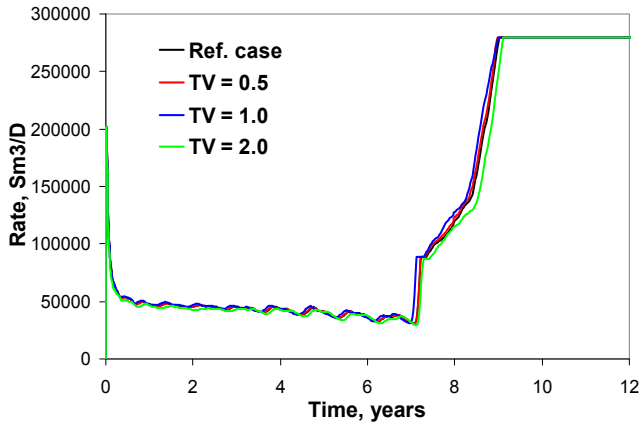

Fig. 17—Field gas rate for three cases with TV = 0.5, 1.0, and 2.0 compared to reference case

The *TV* is used primarily as a convenient parameter with which to summarize results. Conclusions are, however, based on inspection of the individual runs. (The subjective "ranking" of runs was in good agreement with the *TV*-ranking.)

Oil zone

In the reservoir segment in question the oil zone is 13 m thick, and the intuitive definition of the oil zone as 13 equi-thick layers has worked well. Irrespective of the chosen strategy the layers should be defined such that true perforation depths are honored, i.e., at cell centers. Even a deviation of 0.5 m from this principle resulted in a difference in simulated gas break-through of one year. Thinner layers than 1 m did not change the solution noticeably, while 2 m layers above the perforation layer gave results which were noticeable but not significantly different. The reduction in computing time was, however, minimal, so very little was gained by increasing layer thickness in the oil zone.

Gas zone

All runs in this series were done with the same layering below the gas oil contact, hence any differences are due to the gas zone layering strategy alone. This choice of strategy does not seem to matter at all, as both the results and CPU-times were relatively equal in all the studied cases, even using only two layers in the gas cap. A summary of some of the runs is shown in **Table 2**.

This somewhat surprising result can be explained by the gas cap being in expansion mode, such that very little if any of the GOC movement is upwards into the gas zone. The initial gas cap is therefore effectively a one-phase domain. As high resolution primarily is needed in fluid contact areas (two- and three-phase domains), it is sufficient to model the gas zone with coarse cells in this study. This conclusion should not be generalized as it will certainly not be valid in situations where the initial GOC does move upwards.

TABLE 2—TV AND CPU FOR SOME GAS ZONE LAYERING ALTERNATIVES

Strategy (# means "number of")		**TV**	**CPU, sec**
# geo-layers	**# hor-layers (ΔZ, GOC upwards)**		
8	10 (1.5 – 2 – 2.5 – 7x3)	0.43	602
7	7 (1.5 – 2.25 – 3.25 – 4.5 – 3x6)	0.39	573
0	6 (1.6 – 2.6 – 4.1 – 6.6 – 10.5 – 17)	0.40	569
0	4 (2.5 – 5 – 7.5 – 12.5 – 15)	0.44	534
0	2 (8 – 38.5)	0.52	513

Water zone

From experience it is known that the initial OWC on Troll moves both upwards and downwards during production. Hence we should expect that a fine grid is needed in a depth range above and below the initial OWC to capture the contact movement. This was confirmed by the water zone sensitivity batch of runs. All runs in this series were done with identical layering strategy in the gas and oil zones: 8 horizontal layers in the gas zone and 13 in the oil zone.

Table 3 summarizes some of the results from cases with only horizontal layers in the water zone (no geo-layers)

TABLE 3—TV AND CPU FOR SOME WATER ZONE LAYERING ALTERNATIVES (ALL LAYERS HORIZONTAL)

# hor-layers (ΔZ, OWC downwards) (*m* = geometric increase factor)		**TV**	**CPU, sec**
15	(5x1 + 10 layers w. *m* = 1.5)	1.29	243
16	(*m* = 1.25 for all layers)	1.21	235
21	(5x1 + 16 layers w. *m* = 1.25)	1.02	291
24	(1 – 1.25 – 1.5 – 1.75 – 6x2 – 2.5 – 3.1 – 3.9 – 4.9 – 6 – 7.5 ...)	1.15	273
26	(10x1 + 16 layers w. *m* = 1.25)	0.93	372
32	(5x1 – 10x1.5 – 2.25 – 3 – 3.9 – 4.9 – 6 ...)	1.00	361

The total variation is larger than in the gas sensitivity study – none of these cases are particularly good or bad. As expected the best results were achieved when a higher resolution was used near the initial OWC.

As the results from all of the cases with all water zone layers horizontal were only acceptable, but not especially good, the question is whether it is a better strategy to use a hybrid grid in the water zone. (All these cases had relatively thick layers in the deepest parts of the reservoir).

The next batch of runs were sensitivities on distribution of horizontal versus geo-layers in the water zone. In these runs;

- Oil and gas zones were modeled as in the previous batch of runs
- From OWC downwards, ΔZ = 1 m in the top 5 layers, then ΔZ increases by *m* = 1.5 down to the base of the horizontal section
- The deepest part of the water zone was modeled with geo-layers

TABLE 4—TV AND CPU FOR STRATEGIES VARYING TOTAL THICKNESS OF WATER ZONE HORIZONTAL LAYERS				
Hor-grid thickness	**# hor-layers**	**# geo-layers**	**TV**	**CPU, sec**
5	5	56	1.57	497
16.5	9	51	0.78	435
24.5	10	46	0.45	402
32.5	11	40	0.48	367
47.5	12	31	0.63	327
72	13	12	1.02	274
102.5	14	5	1.25	257

Table 4 summarizes some of the results, which are also shown graphically in **Fig. 18**.

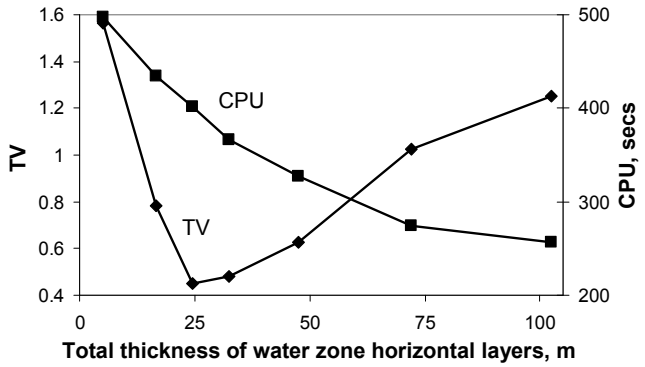

Fig. 18. TV and CPU-time for cases with varying distribution of horizontal vs. geo-layers in the water zone

From these runs, there appears to be an "optimal" thickness of the horizontal grid in the water zone. At least it is clear that "better" results were obtained when using a combination of horizontal and geo-layers, than with horizontal layers only. Intuitively we would perhaps expect that the deepest part of the water zone should act as an "energy tank", where a detailed description was not necessary. However, the runs clearly show that also the deepest parts of the water zone have impact on the flow pattern, probably due to the need for resolving the pressure distribution. The actual dividing line is not critical; from the figure above it would appear that a water zone horizontal grid thickness of about 15–75 m is acceptable, i.e. the horizontal grid covers about 10–45% of the total water zone thickness.

Run Series 5: Some Special Cases

A number of cases were also run to test strategies that may appear promising, but none of these performed any better than the cases presented above. **Table 5** summarizes some examples of the kinds of tests that were done.

TABLE 5—TV AND CPU FOR SOME OTHER SENSITIVITIES		
Strategy	**TV**	**CPU, sec**
Hor. grid only in oil zone, geo-grid for the rest	2.0	588
Geo-grid: top gas cap – 4 m below GOC + entire water zone. 9 hor. layers in rest of oil zone.	2.1	610
As case above, except water zone was optimal hybrid	2.4	563
Hor. grid only for horizontal well layer, geo-grid for the rest	2.3	562
6 equi-thick hor. layers in oil zone ($\Rightarrow$ wells 0.6 m shallower than true depth)	9.5	137

With the exception of the case with erroneous well depth the results were close to acceptable, although not as good as the other cases that were studied. As the computing times were at least of the same order of magnitude as the previous runs, nothing is gained by these alternative strategies.

Conclusions

1. A horizontal grid has better performance than a traditional geo-grid with the same areal resolution
2. Comparable results were obtained from a horizontal grid and a geo-grid with local grid refinement, but computing time for the latter was more than an order of magnitude larger than for the horizontal grid.
3. Horizontal grids can be constructed such that high resolution domains can be defined where most needed, hence increasing computational efficiency.
4. Accurate representation of well completion depths is the most critical factor in thin oil-zone modeling. This is easier achieved on a horizontal grid than on a geo-grid.
5. The horizontal grid performance was acceptable or good for grid cell diameters of up to about 150 m.
6. The layering strategy can be optimized with respect to accuracy and reduced computing time by exploiting the behavior of the gas cap and water zone. This is, however, reservoir dependent.

Nomenclature

GOC	=	gas-oil contact
OWC	=	oil-water contact
LGR	=	local grid refinement
MULTX / Y / Z	=	transmissibility multiplier in *x, y, z* - direction
NNC	=	non-neighbor connection
TV	=	total variation (Eq. 1)
geo-grid	=	grid with layers aligned w. geology
hor-grid	=	grid with true horizontal layers
hybrid grid	=	grid with both geo- and hor. layers
k_n	=	layer n in hor-grid
K_n	=	layer n in geo-grid
m	=	geometric increase factor
KX^{Geo}	=	Permeability along geo-grid x-axis
KX^{Hor}	=	Permeability along hor-grid x-axis

Acknowledgements

The author would like to thank the Troll partnership (ConocoPhillips Skandinavia AS, Petoro AS, A/S Norske Shell, Statoil Petroleum AS, and Total E&P Norge AS) for permission to publish this work. The results and opinions presented in this paper do not necessarily reflect the view of the Troll partnership. Funding and support for the project from Statoil / Troll is highly appreciated.

References

Bowen, G. R. and Leiknes, J. 1995. Parallel Processing Applied to Local Grid Refinement. Paper SPE 30203 presented at Petroleum Computer Conference, Houston, 11–14 June. DOI: 10.2118/30203-MS.

Fantoft, S., Krogh, P. K., and Pollen, S. 1988. Evaluation of Oil Recovery from a Thin Oil Column by a Horizontal Well in the Oseberg Gamma North Reservoir. Paper SPE 18341 presented at SPE European Petroleum Conference, London, 16–19 Oct. DOI: 10.2118/18341-MS.

Henriquez, A., Apeland, O. J., Lie, Ø., and Cheshire, I. 1992. Novel Simulation Techniques Used In a Gas Reservoir With a Thin Oil Zone: Troll Field. *SPERE* **7** (4): 414–418. SPE-21181-PA. DOI: 10.2118/21181-PA.

Hsu, H.-H. 1998. Use of New Horizontal Grids in Reservoir Simulation Models Improve the Chance of Success in Developing Marginal Thin Oil Rim Reservoirs Using Horizontal Wells. Paper SPE 39548 presented at SPE India Oil and Gas Conference and Exhibition, New Delhi, 7–9 April. DOI: 10.2118/39548-MS.

Kabir, C. S., Agamini, M., Holguin, R. A. 2008. Production Strategy for Thin-Oil Coumns in Saturated Reservoirs. *SPEREE* **11** (1). SPE-89755-PA. DOI: 10.2118/89755-PA.

Lien, S. C., Seines, K., Havig, S. O., and Kydland, T. 1991. The First Long-Term Horizontal-Well Test in the Troll Thin Oil Zone. *JPT* **43** (8): 914–917, 970–973. SPE-20715-PA. DOI: 10.2118/20715-PA

Schlumberger, 2009. *ECLIPSE Reference Manual 2009*. Houston: Schlumberger.

Seines, K., Lien, S. C., and Haug, B. T. 1994. Troll Horizontal Well Tests Demonstrate Large Production Potential From Thin Oil Zones. *SPERE* **9** (2): 133–130. SPE-22373-PA. DOI: 10.2118/22373-PA

Thakur, S. C., Bally, K., Therry, D., and Simon, L. 1996. Performance of Horizontal Wells in a Thin Oil Zone Between a Gas Cap and an Aquifer, Immortelle Field, Trinidad. Paper SPE 36752 presented at SPE Annual Technical Conference and Exhibition, Denver, 6–9 Oct. DOI: 10.2118/36752-MS.